ACS Medicinal Chemistry Letters

Open Access
This article is licensed under CC-BY 4.0

pubs.acs.org/acsmedchemlett
Letter

A Nontoxin Aminopyrimidine Probe for Near State-Independent $Na_V1.7$ Inhibition

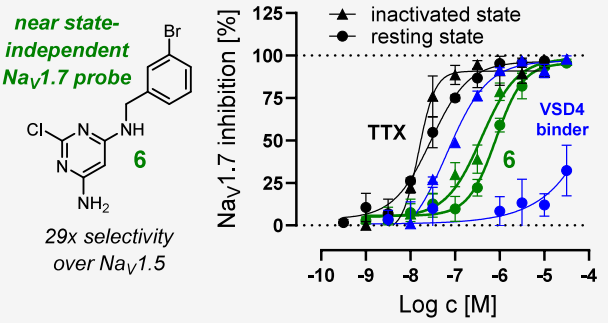
Clemens Dialer,* Marcel Mülbaier, Silke Hagendorf, Inna Slynko, Markus Wagener, Sven Kühnert, Melanie Saldaña Alonso, Clint Young, Cesar Ramirez Molina, Mónica Guberman, David Benjamin Konrad, Florian Jakob, and Stephanie Hennen*

Cite This: ACS Med. Chem. Lett. 2026, 17, 2443−2451

Read Online

ACCESS | Metrics & More | Article Recommendations | Supporting Information

ABSTRACT: The voltage-gated sodium channel $Na_V1.7$ is among the most compelling genetically validated pain targets; however, advanced small-molecule inhibitors, including voltage-sensing domain IV (VSD4)-directed series, have not yet achieved robust clinical efficacy, potentially reflecting pharmacological limitations such as pronounced state dependence. Here, we report a nontoxin aminopyrimidine series that serves as a differentiated pharmacological probe for near state-independent $Na_V1.7$ inhibition. Using a high-throughput automated patch clamp screening cascade designed to deprioritize established local anesthetic pore binders, we identified hit **1** and optimized it to compound **6**, which combines balanced resting- and inactivated-state potency (IC_{50} = 1.00 and 0.45 μM, respectively). It displays a 29-fold selectivity margin over $Na_V1.5$ and a tetrodotoxin (TTX)-like isoform profile that includes comparable activity on $Na_V1.7$ and $Na_V1.1$. Structure−activity studies identified the aminopyrimidine core and methylene-linked aniline motif as key determinants of this profile, while Na_V mutant profiling supports a functional fingerprint consistent with pore-proximal modulation distinct from VSD4-directed inhibition.



KEYWORDS: *$Na_V1.7$ inhibitor, SCN9A, pharmacological probe, near state-independence, tetrodotoxin-like inhibition*

Chronic and severe pain remain a major unmet medical need, and human genetics have identified the voltage-gated sodium channel $Na_V1.7$ (encoded by the gene SCN9A) as an attractive target for nonopioid analgesia.[1,2] Loss-of-function variants in SCN9A cause congenital insensitivity to pain,[3] whereas gain-of-function variants are associated with severe pain syndromes.[4,5] However, translating this genetic validation into clinically effective small-molecule $Na_V1.7$ inhibitors has proven difficult.[6−8]

Many advanced $Na_V1.7$ small-molecule programs have focused on the voltage-sensing domain IV, VSD4,[9] an approach capable of achieving substantial Na_V subtype selectivity. Nevertheless, VSD4-directed inhibitors often display pronounced state dependence with potency strongly influenced by channel gating state. This pharmacological profile may restrict effective target engagement under pathophysiologically relevant firing conditions and has been discussed as one factor contributing to the lack of robust clinical efficacy of $Na_V1.7$ inhibitors.[6] In addition, achieving sufficient exposure at peripheral nociceptive sites, including dorsal root ganglia (DRG), may further constrain this modality.[10,11]

Clinically used local anesthetics, such as lidocaine and tetracaine, demonstrate the analgesic potential of pan-Na_V inhibition, but their broad isoform activity limits their systemic utility.[12] These observations highlight an opportunity for differentiated $Na_V1.7$ modulators that retain small-molecule tractability while reducing the state dependence associated with VSD4-directed binders.[6,13]

A key mechanistic consideration in this context is the channel state dependence. Na_V channels cycle among resting, open, and inactivated conformations during electrical activity, and inhibitor potency can vary markedly across these states. Electrophysiological profiling is therefore essential for distinguishing binding site effects from state-dependent modulation and channel kinetic effects.[14−16] Inhibitors with reduced state dependence are attractive because their activity is less restricted to a particular gating state, offering pharmacology that is mechanistically distinct from classical state-dependent $Na_V1.7$ inhibitors. Such profiles may be supported by targeting

Received: August 12, 2026
Revised: September 25, 2026
Accepted: September 29, 2026
Published: October 14, 2026



ACS Publications
© 2026 The Authors. Published by American Chemical Society

https://doi.org/10.1021/acsmedchemlett.6c00443
ACS Med. Chem. Lett. 2026, 17, 2443−2451

channel regions such as the extracellular outer pore, where accessibility is less affected by gating state transitions than that of regions directly coupled with voltage sensor movement.

Within this environment, Na_V binding site 1 provides a well-defined mechanistic reference point (Figure 1A).[17,18] This site

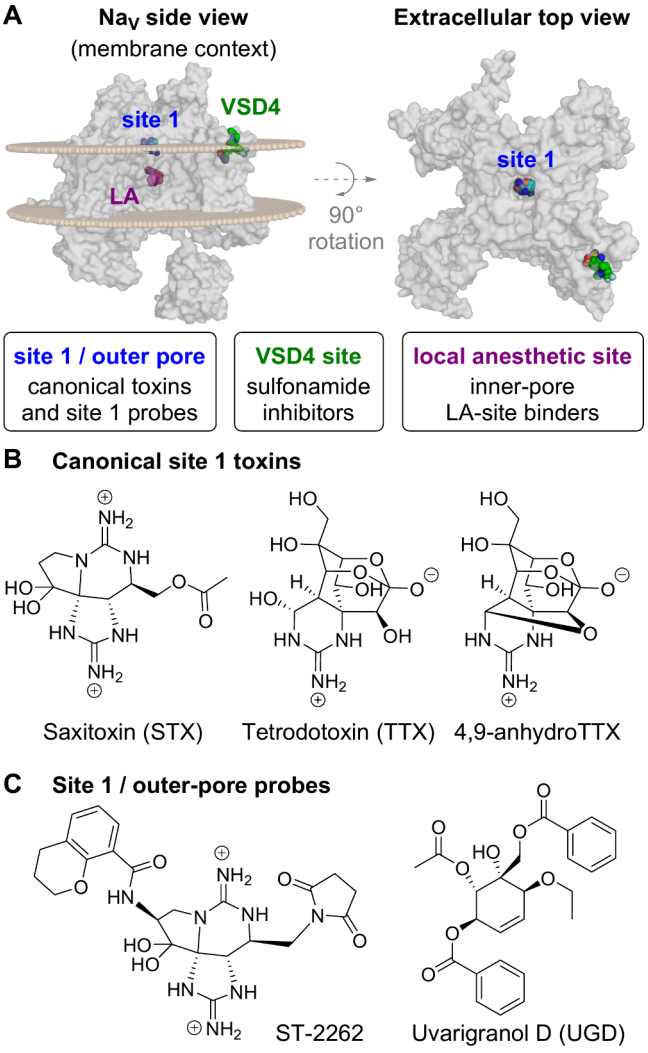


Figure 1. Representative Na_V ligand-binding paradigms. (A) Human $Na_V1.7$ structure in membrane context and extracellular top view (modeled from PDB 7W9P[28]); Nav1.7 is shown as the gray surface and the membrane is shown in beige, highlighting the site 1 pocket/outer-pore region (blue), VSD4 site (green), and local anesthetic (LA) site (magenta). Structural alignment details are provided in the Supporting Information. (B) Canonical state-independent site 1 pore blockers: STX, TTX, and 4,9-anhydroTTX.[19] (C) Representative site 1 probes: ST-2262,[20,21] a $Na_V1.7$-selective site 1 ligand targeting T1398/I1399, and UGD,[24] a T1398-dependent site 1 probe.

is the canonical binding region for guanidinium toxins such as saxitoxin (STX), tetrodotoxin (TTX), and 4,9-anhydroTTX, which produce state-independent pore block (Figure 1B). While these toxins are challenging as therapeutic starting points because of their structural complexity, polarity, and potential off-target liabilities, they provide a valuable framework for understanding state-independent Na_V channel inhibition.[19]

Although Na_V site 1 is highly conserved across isoforms, subtle sequence differences along the extracellular exit vector of the site 1 pocket rather than within the canonical TTX/STX binding locus itself may enable subtype differentiation. In human $Na_V1.7$, residues within the domain III P-loop, including T1398 and I1399, have been implicated in isoform-dependent pharmacology and have motivated efforts to develop site-1-directed ligands. STX-derived analogues from SiteOne Therapeutics, including ST-2262[20,21] (Figure 1C), ST-2530,[22] and ST-2560,[23] further illustrate ongoing efforts to translate site 1 pharmacology into more selective $Na_V1.7$-directed inhibitors. Beyond STX and TTX, uvarigranol D has also been described as an outer-pore/site-1-directed probe with strong interaction on T1398. However, in contrast to high-affinity guanidinium toxins, UGD displays micromolar apparent affinity and retains state-dependent behavior, highlighting the need for chemically tractable probes with differentiated state dependence profiles (Figure 1C).[24]

Here, we report a nontoxin aminopyrimidine series that enables near state-independent inhibition of $Na_V1.7$ and $Na_V1.1$ and provides a chemically tractable pharmacological probe for investigating pore-proximal Na_V modulation. Identified through automated patch clamp screening, this series was optimized to define the structural features required for activity while minimizing state-dependent bias. Because state-independent Na_V inhibition has historically been associated mainly with toxin-derived site 1 ligands, "non-toxin" emphasizes that this electrophysiological profile is achieved with a synthetically accessible scaffold rather than toxin chemistry.

Our high-throughput screening (HTS) strategy was built around the premise that near state-independent $Na_V1.7$ inhibitors would be most effectively identified using a functional electrophysiology-based cascade rather than indirect activity assays (Figure 2). Accordingly, automated patch clamp (APC) electrophysiology[25] was used as a physiologically relevant readout to capture compound activity across resting and inactivated channel states while providing mechanistically informative sodium-current measurements. To further bias the campaign away from conserved pore blockers, the screening cascade incorporated a double local anesthetic site mutant, $Na_V1.7$ F1737A/Y1744A (dLA), thereby deprioritizing compounds acting through the local anesthetic binding region.[26,27] This strategy was intended to reduce rediscovery of non-selective pore binders such as tetracaine and to favor compounds engaging alternative binding environments with the potential to support differentiated $Na_V1.7$ pharmacology. In total, more than 800,000 compounds, including the 508,119-member ESCulab library, were screened by compound pooling (three compounds per well) in CHO cells expressing the dLA $Na_V1.7$ mutant together with auxiliary $\beta1$ and $\beta2$ subunits (Uniprot ID Q125898-3). Following deconvolution, selected hits were retested on wild-type $hNa_V1.7$ to determine IC_{50} values (10-point concentration–response, $n = 2$, $N = 1$), counterscreened against $hNa_V1.5$ for primary selectivity assessment, and subsequently advanced into a broader subtype panel including $Na_V1.1$ and $Na_V1.8$. Promising compounds were then subjected to extended in vitro profiling and mechanistic studies using bespoke $Na_V1.7$ mutants, including the VSD4 mutant R1608A, the TTX-resistant pore mutant Y362S, and the $Na_V1.7$-specific T1398M-I1399D mutant, to distinguish differentiated binding modes and assess potential site 1 engagement.

Tracking compounds with low state bias was a central objective of the campaign because voltage-clamp protocols

https://doi.org/10.1021/acsmedchemlett.6c00443
ACS Med. Chem. Lett. 2026, 17, 2443−2451

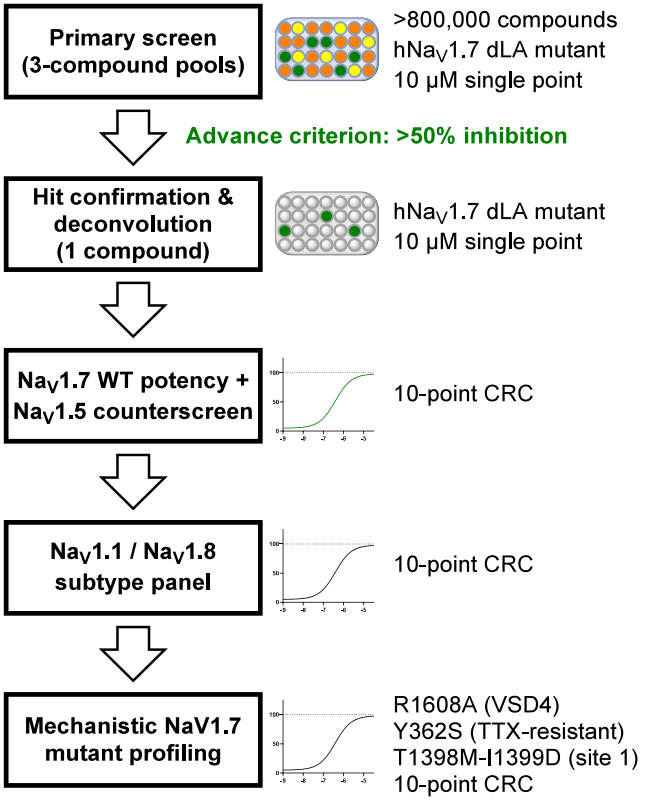


Figure 2. Functional HTS screening cascade used to identify near state-independent $Na_V1.7$ inhibitors by automated patch clamp (APC). Primary screening was performed by 3-compound pooling on $hNa_V1.7$ dLA F1737A/Y1744A, followed by hit confirmation/deconvolution (1 compound), counterscreening, early subtype profiling, and mechanistic mutant profiling. dLA, double local-anesthetic-site mutant; CRC, concentration−response curve.

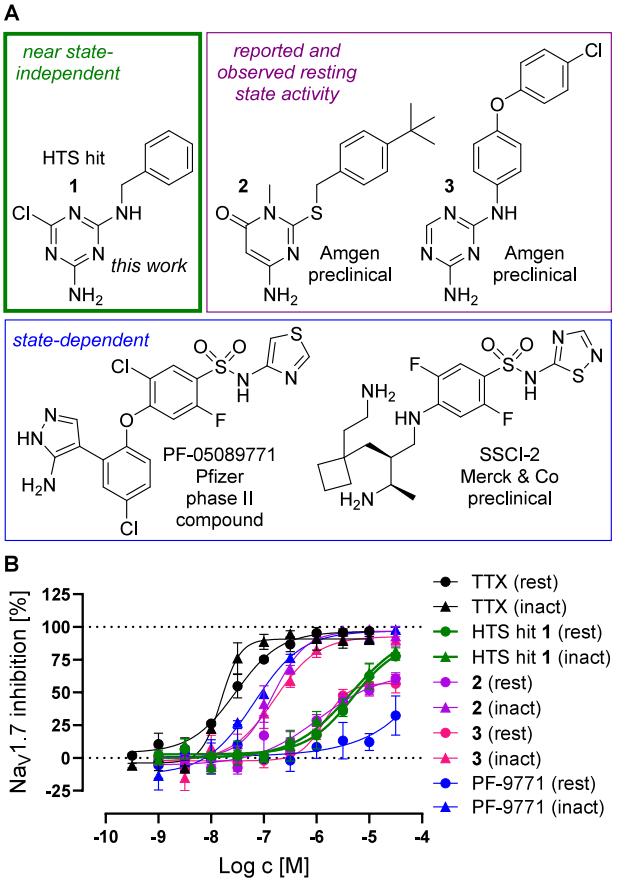


Figure 3. (A) HTS hit **1**, reported Amgen compounds **2**[31] and **3**,[32] and representative VSD4 binder compounds, PF-05089771[29] and SSCI-2.[30] (B) $Na_V1.7$ concentration−response curves using the APC setup for resting (circles) and inactivated (triangles) state inhibition. Data points are shown as mean ± SD from a representative experiment.

remain essential for characterizing Na_V inhibitors and can provide insight into state dependence, use dependence, and block kinetics. At the same time, state dependence in Na_V electrophysiology is inherently protocol-dependent: apparent IC_{50} values can shift substantially with the holding potential and pulse paradigm, complicating direct comparison across studies. Most selective $Na_V1.7$ inhibitors preferentially stabilize inactivated states, whereas truly state-independent blocking is more commonly associated with site 1 pore blockers such as TTX and STX, as well as selected peptide toxins.

Within a single, standardized assay format, however, compound-specific differences in resting versus inactivated state activity remain highly informative and can be used to identify differentiated pharmacological profiles. In this work, we therefore use the term *near state-independent* to describe compounds that show closely balanced resting- and inactivated-state potency within our standardized APC protocol, while recognizing that this classification is assay-dependent and should not be overinterpreted across different electrophysiological formats. Operationally, we define near state-independence as a state-bias ratio (IC_{50}[rest]:IC_{50}[inact]) between 0.3 and 3 under the APC conditions used here. Within this framework, the screening cascade identified hit **1** (Figure 3A) with a nearly state-independent electrophysiological signature. This profile more closely resembled TTX (Figure 3B) and 4,9-anhydroTTX (Figure S6) than typical state-dependent small-molecule inhibitors PF-05089771[29] and SSCI-2.[30] In addition, early Amgen reports on related analogs **2**[31] and **3**,[32] which also showed observable resting-state activity, first drew our attention to this chemotype and motivated their inclusion as benchmarks. The full profiling data set for hit **1** is summarized in Table S2 of the Supporting Information alongside these reference modulators.

Although hit **1** shares structural features with the Amgen compounds **2** and **3**, these precedents did not anticipate the near state-independent profile observed for the present probe series. In our hands, direct transfer of motifs from the Amgen series was not tolerated (e.g., compound **S-2** versus Amgen compound **2**; see Table S2), and straightforward literature-to-lead transposition did not recover the desired pharmacology.

Likewise, a close-in analog search of >200 compounds around hit **1** (Tanimoto similarity ≥ 0.8) across internal and commercial collections failed to identify near neighbors that reproduced its profile, immediately revealing a steep and series-specific SAR. These findings underscored the value of the HTS campaign. While hit **1** partially resembled previously reported chemotypes, subsequent SAR studies showed that its near state-independent $Na_V1.7$ profile arose from a distinct set of structural features.

We therefore pursued a focused medicinal chemistry campaign guided by three design hypotheses (Figure 4). First, we sought to define the structural requirements for

https://doi.org/10.1021/acsmedchemlett.6c00443
ACS Med. Chem. Lett. 2026, 17, 2443−2451

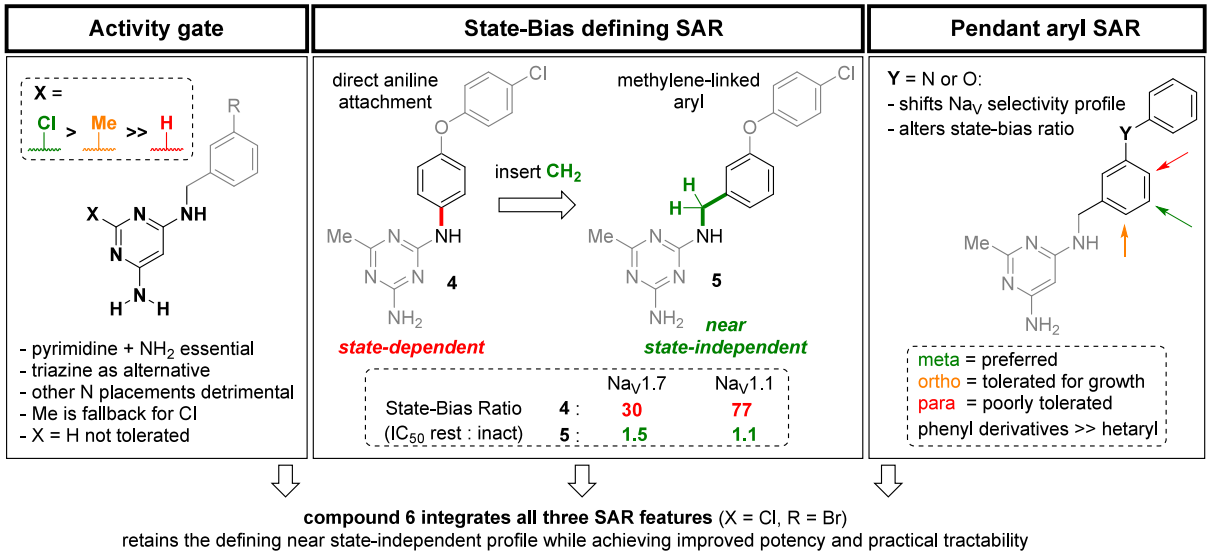


Figure 4. Three-feature SAR map governing activity and probe pharmacology in the aminopyrimidine $Na_V1.7$ series. Activity requires the aminopyrimidine core and exocyclic NH_2 group. State bias is controlled by linker geometry with the methylene-linked aniline motif conferring the desired near state-independent profile relative to direct aniline attachment. The pendant phenyl ring is conformationally and sterically sensitive: meta substitution is preferred, para substitution is poorly tolerated, and ortho/meta positions support limited growth.

activity by varying the heteroaryl core, exocyclic amino group, and substituent X. Second, we investigated whether the geometry of the aniline linkage influenced state bias by comparing directly linked and methylene-spaced analogues. Third, we explored the steric and electronic tolerance of the pendant phenyl ring to determine how substitution affected the potency, state bias, and Na_V isoform profile. The representative analogues synthesized to test these hypotheses are summarized in Table 1. The first design objective was to identify the structural features required to retain Na_V activity (Figure 4, left; Table 1).

To test the influence of the heteroaryl nitrogen pattern, we compared pyrimidine and triazine analogues in matched structural contexts. Pyrimidines **6** and **8** were preferred over the corresponding triazines **9** and **7**, while alternative nitrogen arrangements were generally detrimental (see Supporting Information: **S-1** and **8a**). The exocyclic NH_2 group was also important for activity, and modifications of this functionality were generally not tolerated (data not shown). Finally, the X substituent was varied to determine whether the chloro-substituent could be replaced. Methyl substitution (compound **10**) retained reduced activity and provided a lower-lipophilicity alternative, whereas the unsubstituted (−H) analogue was inactive (data not shown).

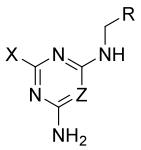
The second design objective was to test whether linker geometry controlled state bias (Figure 4, center). Directly linked compound **4** and methylene-spaced compound **5** were therefore examined as a matched comparison (see Table S2 for activity data). Direct attachment shifted the series toward a pronounced preference for the inactivated state, whereas insertion of a single methylene spacer restored the balanced resting- and inactivated-state profiles observed for hit **1**. Additional substitutions or oxidations at this position were generally detrimental. These findings identified the methylene linker as a key determinant of the near-state-independent pharmacology of the series.

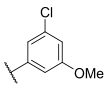
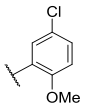
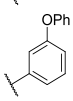
Having established the preferred core and linker, the third design objective was to define the steric and electronic tolerance of the pendant phenyl ring (Figure 4, right; Table 1). Positional isomers (e.g., compounds **12** and **13**) and progressively larger substituents were prepared to distinguish positional and steric effects. Meta substitution was generally preferred; limited growth was tolerated at the ortho and meta positions, and para substitution was poorly tolerated. *O*-Bridged (**14** and **15**) and *NH*-bridged (**16** and **17**) aryl extensions were subsequently examined to explore larger growth vectors and assess whether additional interactions in this region could improve the Na_V isoform profile while retaining potency and low state bias. However, these modifications generally reduced potency, increased state bias, or failed to confer a more favorable isoform profile. Because potency gains were generally accompanied by modest increases in lipophilicity and limited improvements in lipophilic ligand efficiency (LLE),[33] we prioritized potency and profile retention over aggressive physicochemical optimization. This process culminated in compound **6**, which combined improved potency with acceptable early in vitro ADME (Absorption, Distribution, Metabolism, and Excretion) properties and retained the near state-independent profile of the series with IC_{50} values of 1.00 μM and 0.45 μM against resting and inactivated $Na_V1.7$, respectively (Figure 5).

To further define the pharmacology of the series, we compared state-bias ratios of $Na_V1.7$ and $Na_V1.1$ (Figure 6A). Across the probe series, these ratios generally aligned more closely with TTX than with typical small-molecule Na_V inhibitors, which commonly show a pronounced state dependence. Increasing steric bulk on the pendant phenyl ring (e.g., phenol **15** or aniline **17**) selectively eroded resting-state inhibition. Figure 6B extends this comparison across four Na_V isoforms. Here, compound **6** combined the differentiated isoform profile of the series with a 29-fold selectivity margin over $Na_V1.5$, thereby reducing potential liability associated with nonselective Na_V blockers such as tetracaine. Notably, its overall profile mirrored key features of TTX, including a marked preference for $Na_V1.7$ over that of $Na_V1.5$. Importantly, the comparable potency of compound **6** on $Na_V1.1$ and $Na_V1.7$ is not interpreted here as evidence of conventional $Na_V1.7$ subtype selectivity; rather, together with

https://doi.org/10.1021/acsmedchemlett.6c00443
ACS Med. Chem. Lett. 2026, 17, 2443−2451

Table 1. Overview of Structural Modifications and Their Impact on Physicochemical Properties and Potency Across the Probe Series[f]



ID	R	Z	X	IC_{50} $Na_V1.7$[a] [rest; inact]	State-Bias Ratio[b]	Design axis
1		N	Cl	5.28; 4.50[c]	1.2	Screening hit
6		CH	Cl	1.00; 0.45[d]	2.2	Selected Probe
7		N	Cl	1.77; 1.47[d]	1.2	Triazine (8) vs pyrimidine (7)
8		CH	Cl	1.25; 0.54[d]	2.3	Triazine (8) vs pyrimidine (7)
9		N	Cl	1.42; 1.06[d]	1.3	Triazine (9) vs pyrimidine (6)
10		CH	Me	4.79; 1.57[e]	3.1	X= -Cl (6) vs -Me (10)
11		CH	Cl	1.19; 0.60[e]	2.0	Growth vector SAR
12		CH	Cl	2.24; 0.74[e]	3.0	Growth vector SAR
13		CH	Cl	2.13; 0.54[e]	3.9	Growth vector SAR
14		N	Me	5.93; 2.53[d]	2.3	Pendant aryl SAR
15		CH	Me	4.70; 0.76[d]	6.2	Pendant aryl SAR
16		N	Me	8.81; 7.16[d]	1.2	Pendant aryl SAR
17		CH	Me	7.42; 1.63[d]	4.6	Pendant aryl SAR

[a]IC_{50} values were determined using the screening assay protocol described in Supporting Information 2.2.1 and are reported as IC_{50} [rest; inact], where values are independently listed in the order resting state; inactivated state. All values are reported in μM. [b]IC_{50} (rest):IC_{50} (inact). IC_{50} values are reported as geometric means, based on N independent experiments. [c]N = 3. [d]N = 2. [e]N = 1. [f]Extended data are provided in Tables S2 and S3.

the strong $Na_V1.5$ discrimination, it forms part of a TTX-like functional fingerprint that differentiates this probe series from VSD4-directed chemotypes. In contrast, PF-05089771 shows a $Na_V1.7$-selective profile consistent with its VSD4 mechanism, whereas reference modulators **2** and **3** display minimal isoform

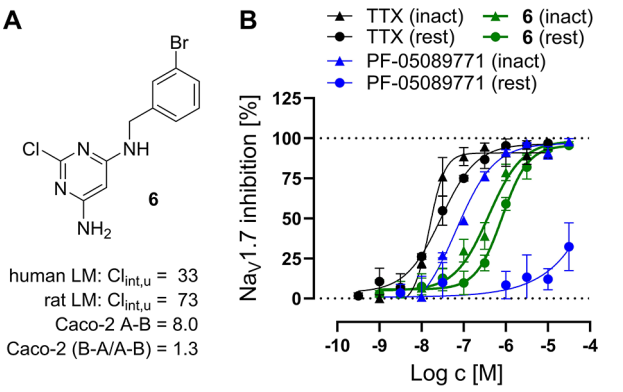


Figure 5. (A) Chemical structure and key *in vitro* ADME properties of compound **6**. (B) APC concentration–response curves for $hNa_V1.7$ inhibition under resting and inactivated conditions. Compound **6** shows a near state-independent profile relative to TTX (state-independent reference) and PF-05089771 (state-dependent VSD4 reference). Data points are mean ± SD from a representative experiment. LM, liver microsomes; $Cl_{int,u}$, unbound intrinsic clearance in [μL/min/mg]; Caco-2, apparent permeability in the A → B and B → A directions in [10^{-6} cm/s].

discrimination, highlighting the distinct profile compared with our probe series.

To further probe the mechanism, we profiled wild-type $Na_V1.7$ and three bespoke $Na_V1.7$ constructs using a dedicated 300-pulse protocol (see SI and Figure S8). This protocol strongly biases engagement of inactivated states and is useful for flagging pulse-train-dependent behavior that is commonly seen with slow-binding inhibitors (e.g., VSD4 binders). Because the paradigm underrepresents resting-state activity, we do not report resting-state potency under these conditions. Under the 300-pulse protocol, known VSD4-directed inhibitors showed pronounced protocol-dependent potency shifts (SSCI-2 ∼ 10-fold; PF-05089771 ∼ 9-fold), consistent with slow equilibration under repetitive pulsing. In contrast, the more advanced aminopyrimidine analogues displayed only minor protocol-dependent differences, a pattern compatible with comparatively rapid equilibration within this assay framework (Figure S8). Importantly, this analysis allows the comparison of mechanistic fingerprints rather than absolute potency alone. In this context, compound **6** does not mimic either classical VSD4 inhibitors or canonical small-molecule pore blockers. Instead, its behavior more closely resembles that of TTX and tetracaine, which likewise show limited sensitivity to the 300-pulse protocol. Definitive conclusions regarding binding kinetics will require future, dedicated kinetic analyses.

Activity was preserved for compounds **6** and **13** on a VSD4 mutant (R1608A)[34] and a TTX-resistant pore mutant (Y362S),[35] arguing against direct VSD4 engagement or reliance on the TTX sensitivity determinant (Figure 6C). Consistent with this, retained potency on $Na_V1.8$ suggests limited dependence on Y362 for binding. On the $Na_V1.7$-specific T1398M-I1399D[24] mutant, compounds **6** and **13** retained activity with little apparent potency shift. Because this construct introduces the corresponding $Na_V1.1$ residues at positions 1398/1399 and compounds **6** and **13** show similar potency on $Na_V1.7$ and $Na_V1.1$, the absence of a mutant effect is consistent with the previously observed isoform profile. In contrast, TTX displayed a modest potency shift. Overall, these functional and mutational fingerprints are consistent with a mode of modulation distinct from established VSD4-directed

https://doi.org/10.1021/acsmedchemlett.6c00443
ACS Med. Chem. Lett. 2026, 17, 2443−2451

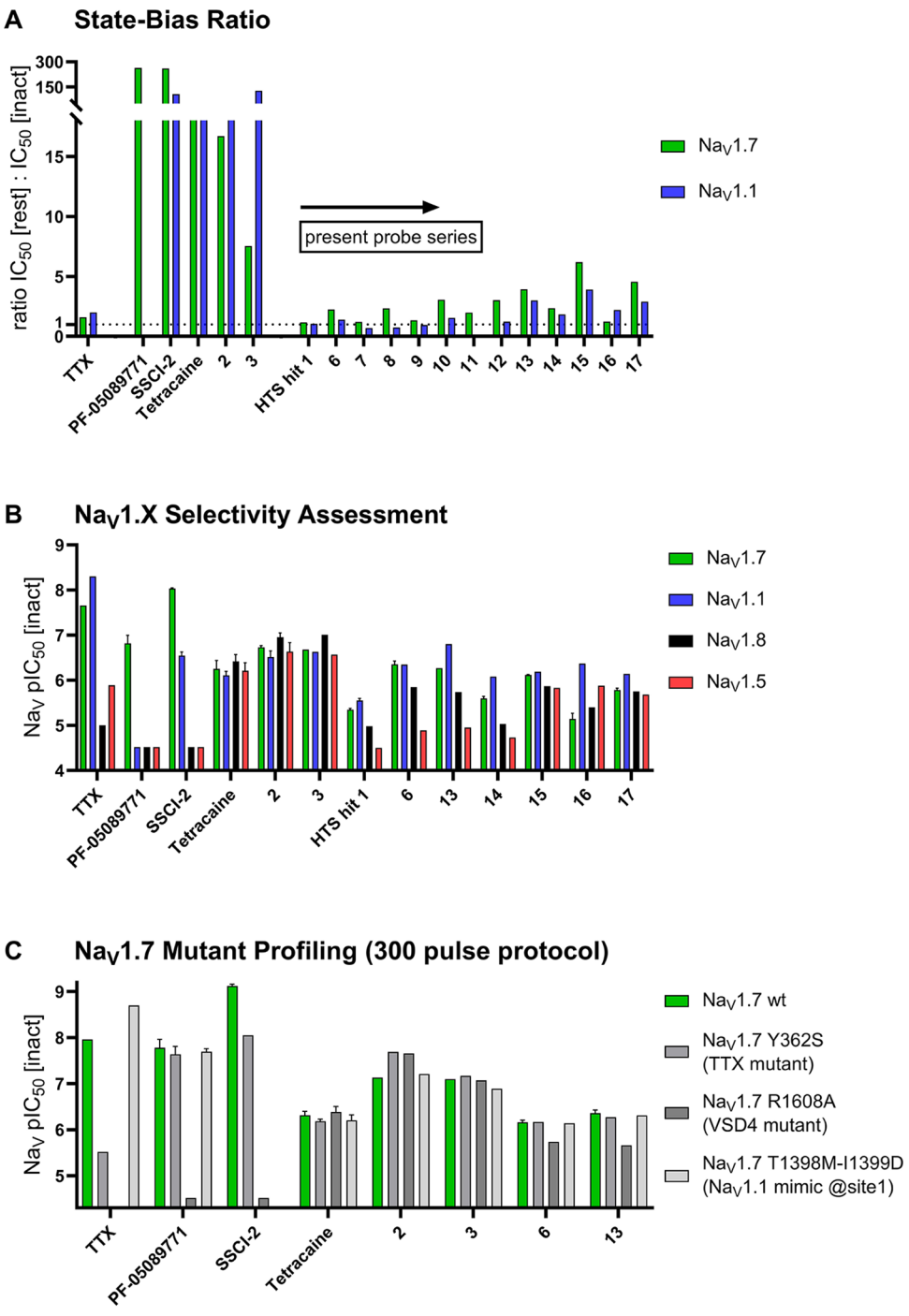


Figure 6. (A) State-bias ratio (IC_{50}[rest]:IC_{50}[inact]) on $Na_V1.7$ and $Na_V1.1$ across benchmark compounds and our series using the screening assay protocol. (B) Selectivity profile of TTX and benchmark Na_V inhibitors compared to our series across four Na_V subtypes—$Na_V1.7$, $Na_V1.1$, $Na_V1.8$, and $Na_V1.5$—(see expanded Figure S7 in SI) using the screening assay protocol. (C) Electrophysiological characterization of the aminopyrimidine series across $Na_V1.7$ wild-type and binding mutants using a bespoke 300-pulse protocol with emphasis on inactivated state. IC_{50} values were determined using 10-point concentration−response curves with each concentration assessed in 2 to 4 replicates. NaV pIC_{50}[inact] values were calculated as $-\log_{10}(Na_V\ IC_{50}[inact])$ with IC_{50} values expressed in mol·L^{-1} (M). Higher pIC_{50} values indicate greater potency. pIC_{50} values are reported as mean ± SD where $N > 1$. Error bars denote SD across independent experiments ($N = 2-5$); bars without error bars correspond to $N = 1$.

inhibition and not dependent on the classical TTX determinant (Y362). While the observed near state-independence and mutant profile are compatible with a pore-proximal mechanism, the current data set cannot unambiguously distinguish classical site 1 engagement from an adjacent vestibular or upper-pore pocket.

Pore-proximal small-molecule interactions are well precedented, spanning local anesthetic-like binding modes as well as structurally characterized pore ligands (e.g., XEN907 and TC-N1752[36]). Structural validation remains pending.

In summary, we report a nontoxin, drug-like pharmacological probe series that enables near state-independent $Na_V1.7$

https://doi.org/10.1021/acsmedchemlett.6c00443
ACS Med. Chem. Lett. 2026, 17, 2443−2451

inhibition, providing practical access to an electrophysiological profile previously associated primarily with toxin-derived ligands. Compound **6** serves as a representative exemplar, combining balanced resting- and inactivated-state potency with a 29-fold selectivity margin over $Na_V1.5$, favorable developability properties, and a TTX-like isoform profile that includes comparable activity on $Na_V1.7$ and $Na_V1.1$. Rather than representing a classical $Na_V1.7$-over-$Na_V1.1$ selective chemotype, this series should be viewed as a mechanistically differentiated probe set for studying alternative mechanisms of Na_V channel modulation. Structure−activity studies identified the aminopyrimidine core and methylene-linked aniline motif as key determinants of the near state-independent phenotype, providing a tractable framework for tuning state dependence within a compact small-molecule scaffold. Functional and mutational profiling further distinguished the series from established VSD4-directed inhibitors and was consistent with a mode of action involving pore-proximal channel modulation, although the precise binding site remains unresolved. Consequently, while the current data are compatible with site 1 engagement, they do not exclude interactions within adjacent vestibular or upper-pore regions. Collectively, these probes provide a differentiated toolkit for exploring mechanisms of sodium-channel modulation beyond established VSD-selective inhibitor classes. Future studies will be required to more comprehensively define the Na_V isoform pharmacology of this probe class.

Safety Statement

No unexpected or unusually high safety hazards were encountered for synthesized compounds. TTX and 4,9-anhydroTTX were handled solely as reference compounds in electrophysiology following standard safety protocols.

■ ASSOCIATED CONTENT

Supporting Information

The Supporting Information is available free of charge at https://pubs.acs.org/doi/10.1021/acsmedchemlett.6c00443.

> Full experimental details for synthesis, NMR data (^{1}H NMR, NOESY), HRMS, elucidation of regioisomerism in lead compounds, electrophysiological methods and activity-profiling protocols, in vitro drug characterization, and computational methods (PDF)

■ AUTHOR INFORMATION

Corresponding Authors

Clemens Dialer − *Grünenthal GmbH, Drug Discovery Engine, 52078 Aachen, Germany*; orcid.org/0000-0002-5659-2776; Email: clemens.dialer@grunenthal.com

Stephanie Hennen − *Grünenthal GmbH, Discovery Biology, 52078 Aachen, Germany*; Email: stephanie.hennen@grunenthal.com

Authors

Marcel Mülbaier − *Grünenthal GmbH, Drug Discovery Engine, 52078 Aachen, Germany*

Silke Hagendorf − *Grünenthal GmbH, Translational Disease Understanding, 52078 Aachen, Germany*

Inna Slynko − *Grünenthal GmbH, Drug Discovery Engine, 52078 Aachen, Germany*

Markus Wagener − *Grünenthal GmbH, Drug Discovery Engine, 52078 Aachen, Germany*; orcid.org/0000-0002-6708-5251

Sven Kühnert − *Grünenthal GmbH, Drug Discovery Engine, 52078 Aachen, Germany*

Melanie Saldaña Alonso − *Grünenthal GmbH, Translational Disease Understanding, 52078 Aachen, Germany*

Clint Young − *GRT Therapeutics, Inc., Cambridge Innovation Center, Cambridge, Massachusetts 02142, United States*

Cesar Ramirez Molina − *Grunenthal Ltd, Maidenhead, Berkshire SL6 8BN, United Kingdom*

Mónica Guberman − *Grünenthal GmbH, Drug Discovery Engine, 52078 Aachen, Germany*

David Benjamin Konrad − *Department of Pharmaceutical Sciences, University of Vienna, 1090 Vienna, Austria*

Florian Jakob − *Grünenthal GmbH, Drug Discovery Engine, 52078 Aachen, Germany*

Complete contact information is available at: https://pubs.acs.org/10.1021/acsmedchemlett.6c00443

Author Contributions

All authors have approved the final version of the manuscript.

Funding

The research was funded by Grünenthal GmbH and its affiliates. The research leading to these results has received support from the Innovative Medicines Initiative 2 Joint Undertaking (JU) under grant agreement No 806948: 'ESCulab: European Screening Centre; Unique Library for Attractive Biology'. The JU receives support from the European Union's Horizon 2020 research and innovation program and EFPIA and Medicines for Malaria Venture (MMV).

Notes

The authors declare no competing financial interest.

■ ACKNOWLEDGMENTS

We gratefully acknowledge the electrophysiology teams at Charles River Laboratories (UK) for their contributions during the conduct of this work, in particular Terry Roberts, Sarah Williams, and Juha Kammonen, as well as Metrion Biosciences (Tony Rush, Marc Rogers) for their expert experimental support. We thank InSCREENex GmbH (Theresa Truschel, Tobias May, Roland Schlucht) for generating the bespoke $Na_V1.7$ mutant cell lines used for mechanistic profiling. We thank Julia Fröhlig for invaluable organizational and operational support throughout the HTS campaign, Sara Reichardt-Ockenfeld for performing the high-resolution mass spectrometry measurements, and Stefanie Peters for conducting and supporting the NMR analyses (all Grünenthal GmbH). We are also grateful to Lyn Rosenbrier Ribeiro and Mauro Marigo (both Grünenthal GmbH) for valuable scientific discussions and insightful feedback throughout the project. We also acknowledge our collaborators at TCG Lifesciences—Shantanu Dutta, Sanjoy Chowdhury, Sarbendu Maiti, Sanjay Katiyar, Anjan Bhunia, Bikash Maity, and their respective teams—for their substantial synthetic contributions to a subset of analogues. We thank Subrata Pandit, Susanta Mondal, Subrata Chattopadhyay, and their teams for conducting *in vitro* ADME profiling. Finally, we thank the chemistry team at Enamine Ltd. (Mykhailo Shafeev, Oleh Salamakha) in Kyiv/Ukraine for their contributions to compound synthesis.

■ ABBREVIATIONS

ADME, absorption−distribution−metabolism−excretion; APC, automated patch clamp; Caco2, A−B permeability in [10^{-6}cm/s]; CHO, Chinese hamster ovary; cLogD, calculated LogD; CNS, central nervous system; dLA, double−local anesthetic (mutant); DRG, dorsal root ganglion; FLIPR, fluorescence imaging plate reader; HEK, human embryonic kidney; HTS, high-throughput screening; hLM, human liver microsomes; hNa_V1.7, human Na_V1.7; IC_{50}, half-maximal inhibitory concentration; inact, inactivated state, LogD, distribution coefficient; LLE, lipophilic ligand efficiency; $Cl_{int,u}$, unbound intrinsic clearance in [μL/min/mg]; MW, molecular weight; *N*, number of independent experiments; *n*, number of technical replicates per concentration; Na_V, voltage-gated sodium channel; PBS, phosphate-buffered saline; PDB, protein database; rest, resting state; SAR, structure−activity relationship; SD, standard deviation; STX, saxitoxin; TTX, tetrodotoxin; UGD, uvarigranol D; VSD, voltage-sensing domain; WT, wild type

■ REFERENCES

(1) Zeng, X.; Powell, R.; Woolf, C. J. Mechanism-Based Nonopioid Analgesic Targets. *J. Clin. Invest.* **2025**, *135* (11), 1.

(2) Waxman, S. G.; Dib-Hajj, S. D. NaV1.7: A Central Role in Pain. *Neuron* **2023**, *111* (17), 2615−2617.

(3) Weiss, J.; Pyrski, M.; Jacobi, E.; Bufe, B.; Willnecker, V.; Schick, B.; Zizzari, P.; Gossage, S. J.; Greer, C. A.; Leinders-Zufall, T.; Woods, C. G.; Wood, J. N.; Zufall, F. Loss-of-Functions in Sodium Channel Nav1.7 Cause Anosmia. *Nature* **2011**, *472* (7342), 186.

(4) Dormer, A.; Narayanan, M.; Schentag, J.; Achinko, D.; Norman, E.; Kerrigan, J.; Jay, G.; Heydorn, W. A Review of the Therapeutic Targeting of SCN9A and Nav1.7 for Pain Relief in Current Human Clinical Trials. *J. Pain Res.* **2023**, *16*, 1487−1498.

(5) Emery, E. C.; Luiz, A. P.; Wood, J. N. Nav1.7 and Other Voltage-Gated Sodium Channels as Drug Targets for Pain Relief. *Expert Opin Ther Targets* **2016**, *20* (8), 975−983.

(6) Eagles, D. A.; Chow, C. Y.; King, G. F. Fifteen Years of NaV1.7 Channels as an Analgesic Target: Why Has Excellent in Vitro Pharmacology Not Translated into in Vivo Analgesic Efficacy? *Br J. Pharmacol Chemother* **2022**, *179* (14), 3592−3611.

(7) Regan, C. P.; Morissette, P.; Kraus, R. L.; Wang, E.; Arrington, L.; Vavrek, M.; de Hoon, J.; Depre, M.; Lodeweyck, T.; Demeyer, I.; Laethem, T.; Stoch, A.; Struyk, A. Autonomic Dysfunction Linked to Inhibition of the Nav1.7 Sodium Channel. *Circulation* **2024**, *149* (17), 1394.

(8) Rothenberg, M.; Tagen, M.; Chang, J.; Boyce-Rustay, J.; Friesenhahn, M.; Hackos, D.; Hains, A.; Sutherlin, D.; Ward, M.; Cho, W. Safety, Tolerability, and Pharmacokinetics of GDC-0276, a Novel NaV1.7 Inhibitor, in a First-in-Human, Single- and Multiple-Dose Study in Healthy Volunteers. *Clin Drug Investig* **2019**, *39* (9), 873−887.

(9) McKerrall; Sutherlin. Nav1.7 Inhibitors for the Treatment of Chronic Pain. *Bioorg. Med. Chem. Lett.* **2018**, *28* (19), 3141−3149.

(10) Yang, J.; Xie, Y.-F.; Smith, R.; Ratté, S.; Prescott, S. A. Discordance between Preclinical and Clinical Testing of NaV1.7-Selective Inhibitors for Pain. *Pain* **2025**, *166*, 481.

(11) Wu, Y.-J.; Guernon, J.; Shi, J.; Ditta, J.; Robbins, K. J.; Rajamani, R.; Easton, A.; Newton, A.; Bourin, C.; Mosure, K.; Soars, M. G.; Knox, R. J.; Matchett, M.; Pieschl, R. L.; Post-Munson, D. J.; Wang, S.; Herrington, J.; Graef, J.; Newberry, K.; Bristow, L. J.; Meanwell, N. A.; Olson, R.; Thompson, L. A.; Dzierba, C. Development of New Benzenesulfonamides as Potent and Selective Nav1.7 Inhibitors for the Treatment of Pain. *J. Med. Chem.* **2017**, *60* (6), 2513−2525.

(12) Körner, J.; Albani, S.; Sudha Bhagavath Eswaran, V.; Roehl, A. B.; Rossetti, G.; Lampert, A. Sodium Channels and Local Anesthetics—Old Friends with New Perspectives. *Front Pharmacol* **2022**, *13*, 837088.

(13) Kitano, Y.; Shinozuka, T. Inhibition of NaV1.7: The Possibility of Ideal Analgesics. *RSC Medicinal Chemistry* **2022**, *13* (8), 895−920.

(14) Catterall, W. A. Structure and Function of Voltage-gated Sodium Channels at Atomic Resolution. *Exp Physiol* **2014**, *99* (1), 35−51.

(15) Lenaeus, M. J.; Gamal El-Din, T. M.; Ing, C.; Ramanadane, K.; Pomès, R.; Zheng, N.; Catterall, W. A. Structures of Closed and Open States of a Voltage-Gated Sodium Channel. *Proc. Natl. Acad. Sci. U. S. A.* **2017**, *114* (15), E3051−E3060.

(16) Lukacs, P.; Pesti, K.; Földi, M. C.; Zboray, K.; Toth, A. V.; Papp, G.; Mike, A. An Advanced Automated Patch Clamp Protocol Design to Investigate Drug—Ion Channel Binding Dynamics. *Front Pharmacol* **2021**, *12*, 738260.

(17) Mulcahy, J. V.; Pajouhesh, H.; Beckley, J.; Delwig, A.; Du Bois, J.; Hunter, J. Challenges and Opportunities for Therapeutics Targeting the Voltage-Gated Sodium Channel Isoform NaV1.7. *J. Med. Chem.* **2019**, *62*, 8695.

(18) Wu, Q.; Huang, J.; Fan, X.; Wang, K.; Jin, X.; Huang, G.; Li, J.; Pan, X.; Yan, N. Structural Mapping of Nav1.7 Antagonists. *Nat. Commun.* **2023**, *14*, 3224.

(19) Nißl, B.; Mülbaier, M.; Grisoni, F.; Trauner, D.; Bermúdez, M.; Dialer, C.; Konrad, D. B. The Chemistry and Biology of the Tetrodotoxin Natural Product Family. *Angew. Chem., Int. Ed. Engl.* **2025**, *64* (35), No. E202502404.

(20) Pajouhesh, H.; Beckley, J. T.; Delwig, A.; Hajare, H. S.; Luu, G.; Monteleone, D.; Zhou, X.; Ligutti, J.; Amagasu, S.; Moyer, B. D.; Yeomans, D. C.; Du Bois, J.; Mulcahy, J. V. Discovery of a Selective, State-Independent Inhibitor of NaV1.7 by Modification of Guanidinium Toxins. *Sci. Rep* **2020**, *10* (1), 14791.

(21) Pajouhesh, H.; Delwig, A.; Beckley, J. T.; Klas, S.; Monteleone, D.; Zhou, X.; Luu, G.; Du Bois, J.; Hunter, J. C.; Mulcahy, J. V. Discovery of Selective Inhibitors of NaV1.7 Templated on Saxitoxin as Therapeutics for Pain. *ACS Med. Chem. Lett.* **2022**, *13* (11), 1763−1768.

(22) Beckley, J. T.; Pajouhesh, H.; Luu, G.; Klas, S.; Delwig, A.; Monteleone, D.; Zhou, X.; Giuvelis, D.; Meng, I. D.; Yeomans, D. C.; Hunter, J. C.; Mulcahy, J. V. Antinociceptive Properties of an Isoform-Selective Inhibitor of Nav1.7 Derived from Saxitoxin in Mouse Models of Pain. *Pain* **2021**, *162* (4), 1250−1261.

(23) Mulcahy, J. V.; Beckley, J. T.; Klas, S. D.; Odink, D. A.; Delwig, A.; Pajouhesh, H.; Monteleone, D.; Zhou, X.; Du Bois, J.; Yeomans, D. C.; Luu, G.; Hunter, J. C. ST-2560, a Selective Inhibitor of the NaV1.7 Sodium Channel, Affects Nocifensive and Cardiovascular Reflexes in Non-human Primates. *Br J. Pharmacol Chemother* **2024**, *181* (17), 3160−3171.

(24) Zhao, F.; Xi, C.; Li, J.; Ren, K.; Tang, Q.; Liang, H.; Yang, S.; Zhu, M. X.; Cao, Z. Molecular Determinant of Low-Voltage Dependence of Human Na v 1.7 Inactivation Revealed by Efficacy-Based Na v 1.7 Selective Inhibitor. *Nat. Commun.* **2026**, *17* (1), 2559.

(25) Bell, D. C.; Dallas, M. L. Using Automated Patch Clamp Electrophysiology Platforms in Pain-related Ion Channel Research: Insights from Industry and Academia. *Br J. Pharmacol Chemother* **2018**, *175* (12), 2312−2321.

(26) Ragsdale, D. S.; McPhee, J. C.; Scheuer, T.; Catterall, W. A. Common Molecular Determinants of Local Anesthetic, Antiarrhythmic, and Anticonvulsant Block of Voltage-Gated Na+ Channels. *Proc. Natl. Acad. Sci. U. S. A.* **1996**, *93* (17), 9270−9275.

(27) Chernov-Rogan, T.; Li, T.; Lu, G.; Verschoof, H.; Khakh, K.; Jones, S. W.; Beresini, M. H.; Liu, C.; Ortwine, D. F.; McKerrall, S. J.; Hackos, D. H.; Sutherlin, D.; Cohen, C. J.; Chen, J. Mechanism-Specific Assay Design Facilitates the Discovery of Nav1.7-Selective Inhibitors. *Proc. Natl. Acad. Sci. U. S. A.* **2018**, *115* (4), E792−E801.

(28) Huang, G.; Liu, D.; Wang, W.; Wu, Q.; Chen, J.; Pan, X.; Shen, H.; Yan, N. High-Resolution Structures of Human Nav1.7 Reveal Gating Modulation through α-π Helical Transition of S6IV. *Cell Rep* **2022**, *39* (4), 110735.

https://doi.org/10.1021/acsmedchemlett.6c00443
ACS Med. Chem. Lett. 2026, 17, 2443−2451

(29) Swain, N. A.; Batchelor, D.; Beaudoin, S.; Bechle, B. M.; Bradley, P. A.; Brown, A. D.; Brown, B.; Butcher, K. J.; Butt, R. P.; Chapman, M. L.; Denton, S.; Ellis, D.; Galan, S. R. G.; Gaulier, S. M.; Greener, B. S.; de Groot, M. J.; Glossop, M. S.; Gurrell, I. K.; Hannam, J.; Johnson, M. S.; Lin, Z.; Markworth, C. J.; Marron, B. E.; Millan, D. S.; Nakagawa, S.; Pike, A.; Printzenhoff, D.; Rawson, D. J.; Ransley, S. J.; Reister, S. M.; Sasaki, K.; Storer, R. I.; Stupple, P. A.; West, C. W. Discovery of Clinical Candidate 4-[2-(5-Amino-1H-Pyrazol-4-Yl)-4-Chlorophenoxy]-5-Chloro-2-Fluoro-n-1,3-Thiazol-4-Ylbenzenesulfonamide (PF-05089771): Design and Optimization of Diaryl Ether Aryl Sulfonamides as Selective Inhibitors of NaV1.7. *J. Med. Chem.* **2017**, *60* (16), 7029−7042.

(30) Kraus, R. L.; Zhao, F.; Pall, P. S.; Zhou, D.; Vardigan, J. D.; Danziger, A.; Li, Y.; Daley, C.; Ballard, J. E.; Clements, M. K.; Klein, R. M.; Holahan, M. A.; Greshock, T. J.; Kim, R. M.; Layton, M. E.; Burgey, C. S.; Serra, J.; Henze, D. A.; Houghton, A. K. Nav1.7 Target Modulation and Efficacy Can Be Measured in Nonhuman Primate Assays. *Sci. Transl Med.* **2021**, *13* (594), No. EAAY1050.

(31) Nguyen, H. N.; Bregman, H.; Buchanan, J. L.; Du, B.; Feric, E.; Huang, L.; Li, X.; Ligutti, J.; Liu, D.; Malmberg, A. B.; Matson, D. J.; McDermott, J. S.; Patel, V. F.; Wilenkin, B.; Zou, A.; McDonough, S. I.; Dimauro, E. F. Discovery and Optimization of Aminopyrimidinones as Potent and State-Dependent Nav1.7 Antagonists. *Bioorg. Med. Chem. Lett.* **2012**, *22* (2), 1055−1060.

(32) Bregman, H.; Nguyen, H. N.; Feric, E.; Ligutti, J.; Liu, D.; McDermott, J. S.; Wilenkin, B.; Zou, A.; Huang, L.; Li, X.; McDonough, S. I.; DiMauro, E. F. The Discovery of Aminopyrazines as Novel, Potent Na″v1.7 Antagonists: Hit-to-Lead Identification and SAR. *Bioorg. Med. Chem. Lett.* **2012**, *22* (5), 2033−2042.

(33) Johnson, T. W.; Gallego, R. A.; Edwards, M. P. Lipophilic Efficiency as an Important Metric in Drug Design. *J. Med. Chem.* **2018**, *61* (15), 6401−6420.

(34) Hackos, D. H.; Ahuja, S.; Mukund, S.; Deng, L.; Khakh, K.; Chang, E.; Young, C.; Lin, S.; Johnson, J. P.; Ortwine, D. F.; Safina, B. S.; Sutherlin, D. P.; Cohen, C. J.; Koth, C. M.; Payandeh, J. Structural Basis of Nav1.7 Inhibition by an Isoform-Selective Small Molecule Antagonist. *Biophys. J.* **2016**, *110* (3), 33A−34A.

(35) Leffler, A.; Herzog, R. I.; Dib-Hajj, S. D.; Waxman, S. G.; Cummins, T. R. Pharmacological Properties of Neuronal TTX-Resistant Sodium Channels and the Role of a Critical Serine Pore Residue. *Pflugers Arch* **2005**, *451* (3), 454−463.

(36) Zhang, J.; Shi, Y.; Huang, Z.; Li, Y.; Yang, B.; Gong, J.; Jiang, D. Structural Basis for NaV1.7 Inhibition by Pore Blockers. *Nat. Struct Mol. Biol.* **2022**, *29* (12), 1208−1216.

https://doi.org/10.1021/acsmedchemlett.6c00443
ACS Med. Chem. Lett. 2026, 17, 2443−2451